11-23-2015

Self-consistent Modeling of Photoionization and the Kerr Effect in Bulk Solids

Jeremy R. Gulley
Kennesaw State University, jgulley@kennesaw.edu

Thomas E. Lanier
Kennesaw State University, tlanier6@kennesaw.edu

Self-consistent modeling of photoionization and the Kerr effect in bulk solids

Jeremy R. Gulley* and Thomas E. Lanier

Department of Physics, Kennesaw State University, Kennesaw, GA, 30144, USA

ABSTRACT

In calculations of ultrafast laser-induced ionization the treatment of fundamental mechanisms such as photoionization and the Kerr effect are treated in isolation using monochromatic perturbative approaches. Such approaches are often questionable for pulses of ultrashort duration and multi-chromatic spectra. In this work we address this issue by solving the quantum optical Bloch equations in a 3D quasi-momentum space and show how to couple this model to ultrashort pulse propagation in dielectrics. This approach self-consistently couples a quantum calculation of the photoionization yield, the photoionization current, and the current from free-carriers with the traditional Kerr effect (self-focusing and self phase modulation) without resort to a perturbative treatment. The material band structure is taken in the tight binding limit and is periodic in the crystal momentum space. As this model makes no assumption about the pulse spectrum, we examine the laser-material interaction of strongly chirped pulses and multi-color multi-pulse schemes of laser-induced material modification. These results are compared to those predicted by standard treatments, such as the Keldysh model of photoionization, for pulses of ultrashort duration.

Keywords: Ultrashort laser pulse propagation, Kerr effect, Photoionization, Self-focusing, Laser-induced ionization, Multi-chromatic pulse, Optical Bloch equations

1. INTRODUCTION

Ultrashort laser pulses have been widely used to study the onset of laser-induced damage.[1–5] One major advantage of such pulses is that their short duration can avoid the onset of thermal effects while the pulse is in transit through the material. Another advantage is that the femtosecond is on the time scale of processes found within the atom, making ultrashort pulses ideal to study the details of fast interactions that are typically time-averaged. However, the spectrum of an ultrashort pulse is not truly monochromatic. It follows that ultrashort pulses will not always interact with a material analogously to a longer pulse whose frequency is well defined. In calculating laser material interactions, this fact is typically ignored in the interest of simplicity. This is consequential in the case of ionization,[5–7] but it is also important for other areas of nonlinear optics.[8,9] In particular, for dielectrics the Kerr effect ceases to be well approximated as an instantaneous contribution to the polarization when the laser frequency approaches a two-photon resonance of the material.[10,11]

Emerging applications and interests in the areas of multi-color laser-machining,[5,12,13] high harmonic generation (HHG),[14–16] and pulse filamentation[17,18] have necessitated a deeper understanding of the fundamental processes in ultrafast laser-material interactions while maintaining a computational simplicity sufficient to simultaneously model pulse propagation through the medium. In this proceedings paper, we explore a simple yet comprehensive model of ultrafast laser material interaction for ultrashort and multi-color pulses. It is intended to give a qualitative and computationally efficient description of linear, nonlinear, and ionization effects in an approximately collisionless medium. The possible role of collisions, being approximated by dephasing rates, can be easily included in the model.

Further author information: (Send correspondence to J. R. G)
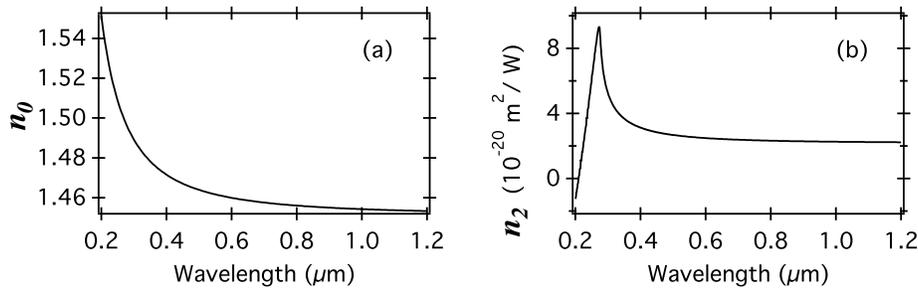Jeremy R. Gulley: E-mail: jgulley@kennesaw.edu, Telephone: 1 470 578 2933

Figure 1. The calculated linear (a) and nonlinear (b) refractive indices as functions of laser wavelength.

2. PHYSICAL MODEL

The electron dynamics under the dipole approximation are often described by the semiconductor Bloch equations.[16] In the limit of a collisionless medium the semiconductor Bloch equations reduce to the optical Bloch equations (OBEs) where the effects of collisions on the polarization are approximated by dephasing rates.[19] For a three band model the equations for this system can be expressed as[15]

$$\frac{dn_{v,\mathbf{k}}}{dt} = -\frac{2}{\hbar}\text{Im}\left[\mathbf{d}_{cv,\mathbf{k}}^* \cdot \mathbf{E}(t)\, P_{vc,\mathbf{k}}\right] + \frac{|e|}{\hbar}\mathbf{E}(t) \cdot \nabla_{\mathbf{k}} n_{v,\mathbf{k}}, \tag{1}$$

$$\frac{dn_{c,\mathbf{k}}}{dt} = -\frac{2}{\hbar}\text{Im}\left[\mathbf{d}_{cv,\mathbf{k}} \cdot \mathbf{E}(t)\, P_{vc,\mathbf{k}}^* + \mathbf{d}_{c'c,\mathbf{k}}^* \cdot \mathbf{E}(t)\, P_{cc'\mathbf{k}}\right] + \frac{|e|}{\hbar}\mathbf{E}(t) \cdot \nabla_{\mathbf{k}} n_{c,\mathbf{k}}, \tag{2}$$

$$\frac{dn_{c',\mathbf{k}}}{dt} = -\frac{2}{\hbar}\text{Im}\left[\mathbf{d}_{c'c,\mathbf{k}} \cdot \mathbf{E}(t)\, P_{cc',\mathbf{k}}^*\right] + \frac{|e|}{\hbar}\mathbf{E}(t) \cdot \nabla_{\mathbf{k}} n_{c',\mathbf{k}}, \tag{3}$$

where $n_{v,\mathbf{k}}$, $n_{c,\mathbf{k}}$, $n_{c',\mathbf{k}}$ are the electron occupation numbers at the quasi-momentum vector $\mathbf{k}$ for the valence (v), first conduction (c), and second conduction (c') bands, respectively. Here, $P_{ij,\mathbf{k}}$ is the coherence between the i and j bands and $\mathbf{d}_{ij,\mathbf{k}}$ is the corresponding dipole matrix element. Only vertical transitions in the quasi-momentum space are assumed. The evolution of the coherences between the various bands are expressed as:

$$\frac{\partial P_{vc,\mathbf{k}}}{\partial t} = -\frac{i}{\hbar}\left(\epsilon_{\mathbf{k}}^{cv} + i\hbar\gamma\right) P_{vc,\mathbf{k}} + \frac{i}{\hbar}\left(n_{v,\mathbf{k}} - n_{c,\mathbf{k}}\right)\mathbf{d}_{cv,\mathbf{k}} \cdot \mathbf{E}(t) + \frac{|e|}{\hbar}\mathbf{E}(t) \cdot \nabla_{\mathbf{k}} P_{vc,\mathbf{k}} + \frac{i}{\hbar}\mathbf{d}_{c'c,\mathbf{k}}^* \cdot \mathbf{E}(t) P_{vc',\mathbf{k}} \tag{4}$$

$$\frac{\partial P_{cc',\mathbf{k}}}{\partial t} = -\frac{i}{\hbar}\left(\epsilon_{\mathbf{k}}^{c'c} + i\hbar\gamma\right) P_{cc',\mathbf{k}} + \frac{i}{\hbar}\left(n_{c,\mathbf{k}} - n_{c',\mathbf{k}}\right)\mathbf{d}_{c'c,\mathbf{k}} \cdot \mathbf{E}(t) + \frac{|e|}{\hbar}\mathbf{E}(t) \cdot \nabla_{\mathbf{k}} P_{cc',\mathbf{k}} - \frac{i}{\hbar}\mathbf{d}_{cv,\mathbf{k}}^* \cdot \mathbf{E}(t) P_{vc',\mathbf{k}} \tag{5}$$

$$\frac{\partial P_{vc',\mathbf{k}}}{\partial t} = -\frac{i}{\hbar}\left(\epsilon_{\mathbf{k}}^{c'v} + i\hbar\gamma\right) P_{vc',\mathbf{k}} + \frac{|e|}{\hbar}\mathbf{E}(t) \cdot \nabla_{\mathbf{k}} P_{vc',\mathbf{k}} - \frac{i}{\hbar}\mathbf{d}_{cv,\mathbf{k}} \cdot \mathbf{E}(t) P_{cc',\mathbf{k}} + \frac{i}{\hbar}\mathbf{d}_{c'c,\mathbf{k}} \cdot \mathbf{E}(t) P_{vc,\mathbf{k}}. \tag{6}$$

In the above equations, the interband dipole matrix elements are related to the momentum matrix elements by $\mathbf{d}_{i \neq j,\mathbf{k}} = -i\hbar\,|e|\,\mathbf{p}_{i \neq j,\mathbf{k}}/(m_0 \epsilon_{ij,\mathbf{k}})$, whereas the intraband dipole elements are accounted for by the terms including the k-space gradients.[15] Furthermore, we assume negligible dipole coupling between the valence and the upper conduction band, i.e. $\mathbf{d}_{vc',\mathbf{k}} \approx 0$. The dephasing rate γ is also assumed to be zero, but can easily be changed to approximate the effects of collisions. In this work the band structure is approximated when calculating the transition energies by $\epsilon_{\mathbf{k}}^{cv} = \epsilon_{\text{gap}} + \sum_{n=\{x,y,z\}}[\Delta_n - \Delta_n \cos(k_n d_n)]$, $\epsilon_{\mathbf{k}}^{c'v} = \epsilon_{\text{sep}} + 2\sum_{n=\{x,y,z\}}(\Delta_n)$, and $\epsilon_{\mathbf{k}}^{c'c} = \epsilon_{\mathbf{k}}^{c'v} - \epsilon_{\mathbf{k}}^{cv}$. Here, the coefficient $\Delta_n = \hbar^2/(m_n d_n^2)$, d_n is the lattice constant of the material in the nth spatial dimension, and m_n is the reduced effective mass for that dimension. When one chooses $d_x = d_y = d_z$, this type of band structure is simple cubic in nature. We note that it has been used to qualitatively model the electron dynamics of solids,[20, 21] and has also been used in weighted combinations to model more realistic crystal structures.[14, 15]

To obtain both linear and nonlinear optics consistent with many optical glasses, we select values of $d_x = d_y = d_z = 0.26$ nm, $d_{i \neq j,\mathbf{k}=0} = -i1.76 \times 10^{-29}$ C m, and $m_x = m_y = m_z = 0.43\,m_e$, where m_e is the rest
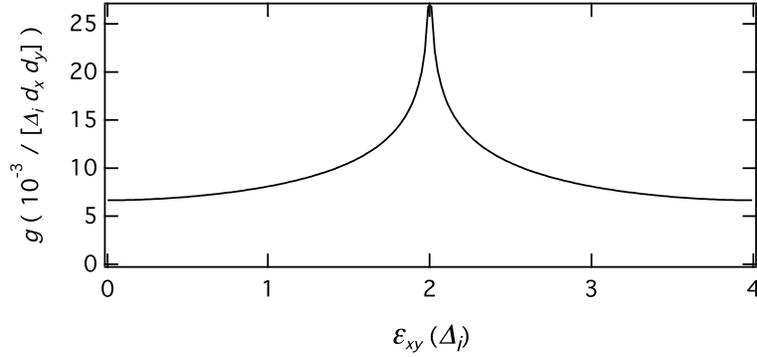
Figure 2. The 2D density of states for a simple cubic tight-binding band structure.

electron mass. The energy separation between the top of the first conduction band and the bottom of the second conduction band is assumed to be $\epsilon_{\mathrm{sep}} = 0.1$ eV. The linear and nonlinear refractive indices associated with these values and our chosen band structure can be calculated by a quantum sum over states and are shown in Fig. 1.

The electric field $\mathbf{E}(t)$ is assumed to be linearly polarized in the z direction. Under these conditions, the solving of Equations (1)-(6) in the full 3D momentum space can be simplified for our chosen band structure by making the coordinate transformation $\{k_x, k_y, k_z\} \rightarrow \{\epsilon_{xy}, k_z\}$. Here, the transverse energy coordinate ϵ_{xy} contains all of the quasi-momentum dependence for directions normal to the field polarization. The density of states under this new coordinate system is shown in Fig. 2 as a function of ϵ_{xy}. Note that this density of states is constant for all k_z. Under the new coordinates, the total ionization, total polarization, and the free-current density as functions of time are calculated by integrating over the first Brillouin zone and summing over the bands.

$$N_c = \sum_{i=c,c'} \int_{\mathbf{BZ}} n_c(\varepsilon_{xy}, k_z) \, g(\varepsilon_{xy}, k_z) \, d\varepsilon_{xy} \, dk_z, \tag{7}$$

$$\vec{P} = \sum_{i \neq j} \int_{\mathbf{BZ}} \vec{d}_{ij}(\varepsilon_{xy}, k_z) \, P_{ij}(\varepsilon_{xy}, k_z) \, g(\varepsilon_{xy}, k_z) \, d\varepsilon_{xy} \, dk_z, \tag{8}$$

$$\vec{J}_f = \sum_{i} \int_{\mathbf{BZ}} -e \, n_i(\varepsilon_{xy}, k_z) \, \vec{v}_i(\varepsilon_{xy}, k_z) \, g(\varepsilon_{xy}, k_z) \, d\varepsilon_{xy} \, dk_z, \tag{9}$$

where $\vec{v}_i = (1/\hbar)\nabla_{\mathbf{k}}\varepsilon_{i,\mathbf{k}}$. The results of solving this system of equations for ultrashort and multi-color pulse systems are shown below. This change of coordinates reduces the time required for the full 3D momentum space calculation from days to minutes.

3. RESULTS

For exposure to a 800 nm, 20 fs pulse with a peak intensity of 10 TW/cm^2, Fig. 3 shows the final occupation numbers in the first conduction band as a function of ϵ_{xy} and k_z. Here one can see the evidence of multi-photon absorption in the various rungs of the final electron distribution. We note that there were also electrons in the second conduction band, albeit with occupation numbers an order of magnitude or less than those of the first conduction band. The corresponding nonlinear polarization for this pulse is shown in Fig. 4. Also shown in Fig. 4 is the calculation of the traditional Kerr effect $P_{\mathrm{Kerr}}(t) = \epsilon_0 \chi^{(3)} E^3(t)$. The agreement between the two models is initially good. As ionization increases, however, the emergence of higher harmonics becomes evident in the full calculation. Figure 5(a) shows the full current density calculation along with the classical free current density calculated by $J_c(t) = (e^2/m_r) \int_{-\infty}^{t} E(t) N_k(t) dt$, where $N_k(t)$ is the ionization yield calculated by the Keldysh model.[22] Figure 5(b) show the time integrated values of both quantities in Figure 5(a) so that they
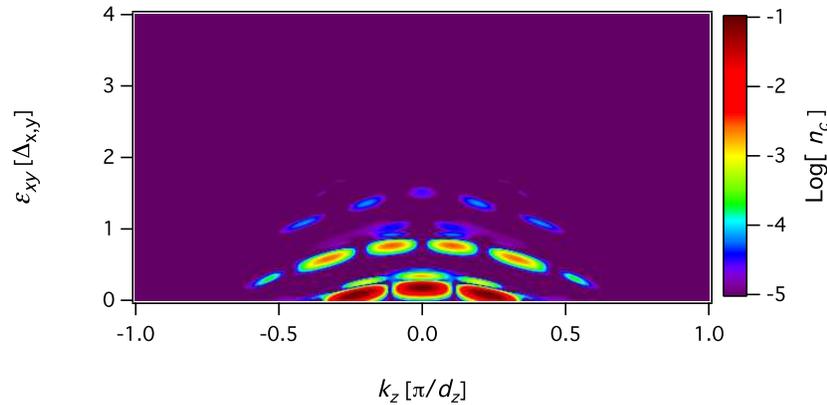
Figure 3. The occupation probability n_c as a function of the transverse energy ϵ_{xy} and the field-polarized momentum k_z after exposure to a 20 fs, 800 nm laser pulse.
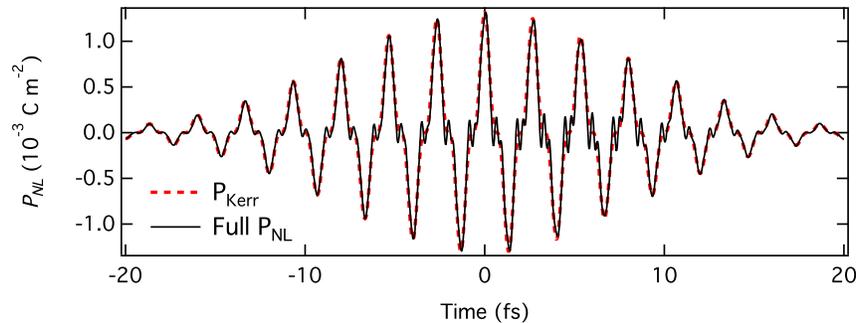

Figure 4. The calculated nonlinear polarization (solid-black line) and the traditional Kerr-type polarization (dashed-red line) during exposure to a 20 fs, 800 nm laser pulse.

appear as polarization contributions. Note that initially the full free polarization makes a contribution that is, in form, indistinguishable from the ordinary Kerr effect. Only after ionization occurs does the full free current match the form of the classical current, which in turn leads to plasma defocusing of a laser beam.

Figure 6 shows the ionization yields for 50 fs single and multi-color pulse combinations: for a 800 nm pulse of peak intensity 7.5 TW/cm^2 (shown in red), a 267 nm pulse of peak intensity 2.5 TW/cm^2 (shown in purple), and both pulses present simultaneously (shown in green). All the pulses are assumed to be Gaussian and centered about $t = 0$. Figure 7 shows the analogous results, but with the 267 nm pulse (third harmonic) replaced with a 400 nm pulse (second harmonic) of the same pulse width and intensity. In each case the conduction electron population oscillates with time according to the field by absorption and stimulated emission (purely adiabatic transitions). Only after the pulse is gone does it become clear what the final ionization yield is. Out of all the individual pulses, the 267 nm pulse has the highest yield in isolation, despite being one-third the intensity of the 800 nm field. This is due to its higher multi-photon ionization probability. Once the fields are combined, the resulting yield increases by an order of magnitude, which is much more than simply adding the ionization yields of the two individual pulses, as is sometimes done in the literature.[5] This fact is even more pronounced once the 267 nm pulse is switched with an otherwise 400 nm pulse in Fig. 7. These results demonstrate the importance of multi-chromatic field interference effects when multiple pulses are present simultaneously. A simple rate equation approach of adding the ionization yields of two individual pulses together can underestimate the total yield by well over an order of magnitude if the delay between the pulses is not sufficiently large.
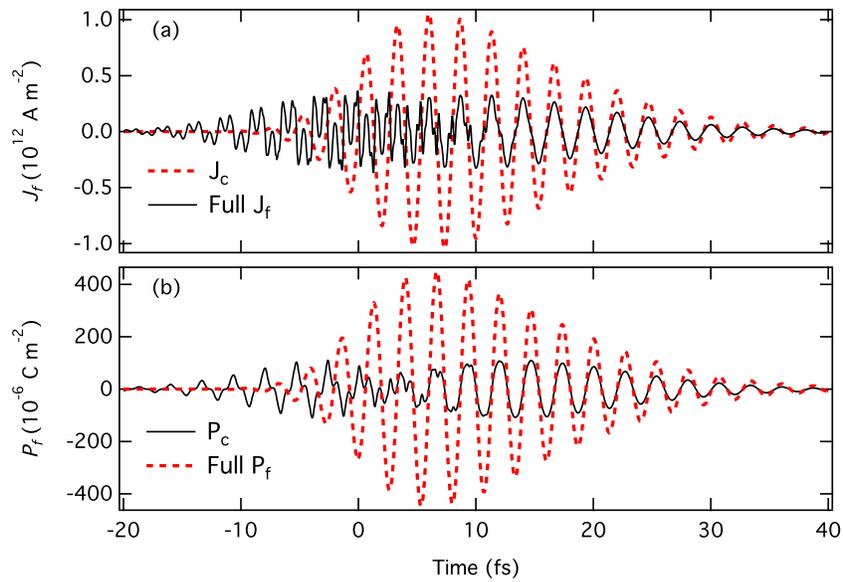
Figure 5. The calculated free current densities (a) and polarizations (b) as calculated by the OBEs (solid-black lines) and the classical free charge current (dashed-red line) during exposure to a 20 fs, 800 nm laser pulse.
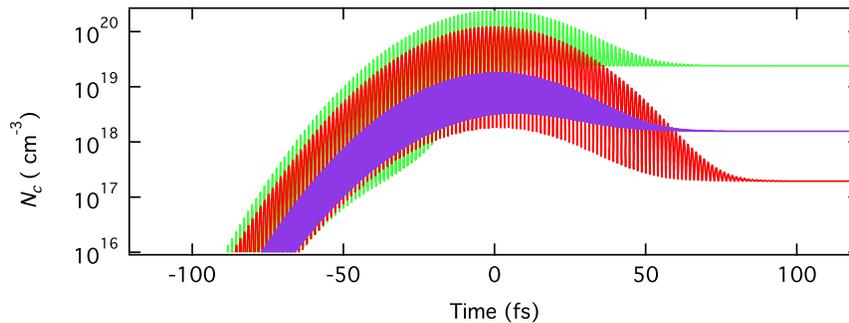

Figure 6. The total conduction band populations N_c as a function of time for 50 fs pulses of wavelengths 800 nm (red line, $I_{\mathrm{peak}} = 10$ TW/cm^2), 267 nm (purple line, $I_{\mathrm{peak}} = 2.5$ TW/cm^2), and both pulses combined (green line).
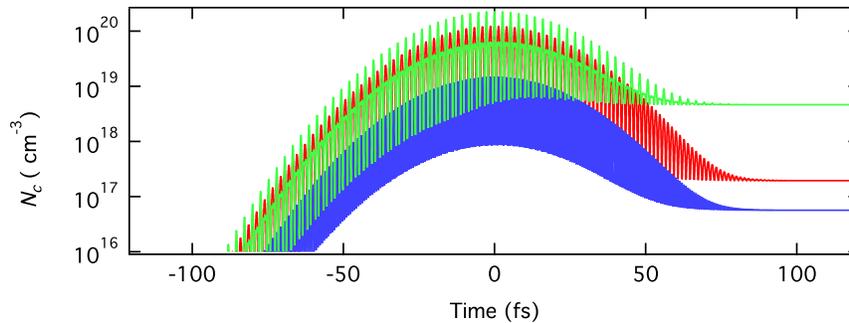

Figure 7. The total conduction band populations N_c as a function of time for 50 fs pulses of wavelengths 800 nm (red line, $I_{\mathrm{peak}} = 10$ TW/cm^2), 400 nm (purple line, $I_{\mathrm{peak}} = 2.5$ TW/cm^2), and both pulses combined (green line).

4. DISCUSSION

The results in Figs. 3-5 collectively suggest that the traditional separation of ionization calculations from those of nonlinear optical effects is not generally appropriate for ultrashort pulses. The multi-chromatic results in Figs. 6 and 7 additionally suggest that simplified rate equation approaches that add multi-photon ionization rates from individual pulses that are simultaneously present can make errors of an order of magnitude or greater. With these facts in mind, it is also important to remember the qualitative nature of the model that we have used in this work. A simple cubic band structure for a three band system was used to model materials generally possessing more complicated crystal structures. Thus the presented results are also of a qualitative nature, but they give insight into processes of importance not just to laser-induced damage of dielectrics, but also to high harmonic generation and pulse filamentation in solids. Furthermore, by reducing the full 3D momentum space into an effective 2D system of equations, such calculations can be performed on time-scales sufficient to couple with pulse propagation simulations. If extended to account for more complicated crystals (additional bands and more realistic band structures) this approach can self-consistently couple the ionization and nonlinear optical calculations of ultrashort pulses in many solids of interest.

5. CONCLUSION

Calculations of ultrafast laser-induced ionization and nonlinear optical effects, such as the Kerr effect, are typically treated in isolation using monochromatic perturbative approaches. This simplification is often necessary due to the lack of knowledge of the detailed material properties, or for computational reasons. However, this approach is not valid for pulses of ultrashort duration and multi-chromatic spectra. The quantum optical Bloch equations in a 3D quasi-momentum space can be reduced to an effective 2D system of equations that can be coupled to ultrashort pulse propagation in dielectrics. The material band structure is taken in the tight binding limit and is periodic in the quasi-momentum space. Such an approach calculates the contributions of photoionization, the Kerr effect, and current from free carriers in a self-consistent way that makes no assumptions about the pulse spectrum. It provides an efficient mechanism to qualitatively study laser-material interactions important to laser-induced damage and many other active areas of research. In particular, photoionization and the Kerr effect are shown to be strongly coupled for ultrashort pulses on the order of 20 fs or less, contrary to the predictions of more traditional approaches. The comparisons of ionization yields for ultrashort pulses of different colors, both combined and in isolation, further demonstrate the need for such models in advancing our understanding of multi-chromatic approaches to laser-induced modifications of solids.

ACKNOWLEDGMENTS

REFERENCES

[1] Tien, A.-C., Backus, S., Kapteyn, H., Murnane, M., and Mourou, G., "Short-pulse laser damage in transparent materials as a function of pulse duration," *Phys. Rev. Lett.* **82**, 3883–3886 (May 1999).

[2] Chen, J. K., Tzou, D. Y., and Beraun, J. E., "Numerical investigation of ultrashort laser damage in semiconductors," *Intern. J. Heat Mass Trans.* **48**, 501–509 (Jan-Feb 2005).

[3] Sudrie, L., Franco, M., Prade, B., and Mysyrowicz, A., "Study of damage in fused silica induced by ultrashort ir laser pulses," *Opt. Comm.* **191**(3-6), 333 – 339 (2001).

[4] Englert, L., Rethfeld, B., Haag, L., Wollenhaupt, M., Sarpe-Tudoran, C., and Baumert, T., "Control of ionization processes in high band gap materials via tailored femtosecond pulses," *Opt. Express* **15**, 17855–17862 (Dec 2007).

[5] Yu, X., Bian, Q., Zhao, B., Chang, Z., Corkum, P. B., and Lei, S., "Near-infrared femtosecond laser machining initiated by ultraviolet multiphoton ionization," *Appl. Phys. Lett.* **102**(10), 101111 (2013).

[6] Duchateau, G. and Bourgeade, A., "Influence of the time-dependent pulse spectrum on ionization and laser propagation in nonlinear optical materials," *Phys. Rev. A* **89**, 053837 (May 2014).

[7] Louzon, E., Henis, Z., Pecker, S., Ehrlich, Y., Fisher, D., Fraenkel, M., and Zigler, A., "Reduction of damage threshold in dielectric materials induced by negatively chirped laser pulses," *Appl. Phys. Lett.* **87**(24), 241903 (2005).

[8] Korbman, M., Kruchinin, S. Y., and Yakovlev, V. S., "Quantum beats in the polarization response of a dielectric to intense few-cycle laser pulses," *New J. of Phys.* **15**(1), 013006 (2013).

[9] Roppo, V., Akozbek, N., de Ceglia, D., Vincenti, M. A., and Scalora, M., "Harmonic generation and energy transport in dielectric and semiconductors at visible and uv wavelengths: the case of gap," *J. Opt. Soc. Am. B* **28**, 2888–2894 (Dec 2011).

[10] Sheik-Bahae, M., Hutchings, D., Hagan, D., and Van Stryland, E., "Dispersion of bound electron nonlinear refraction in solids," *IEEE J. Quantum Electron.* **27**, 1296–1309 (Jun 1991).

[11] Christodoulides, D. N., Khoo, I. C., Salamo, G. J., Stegeman, G. I., and Stryland, E. W. V., "Nonlinear refraction and absorption: mechanisms and magnitudes," *Adv. Opt. Photon.* **2**, 60–200 (Mar 2010).

[12] Bityurin, N. and Kuznetsov, A., "Use of harmonics for femtosecond micromachining in pure dielectrics," *J. Appl. Phys.* **93**(3), 1567–1576 (2003).

[13] Yu, X., Bian, Q., Chang, Z., Corkum, P. B., and Lei, S., "Femtosecond laser nanomachining initiated by ultraviolet multiphoton ionization," *Opt. Express* **21**(20), 24185–24190 (2013).

[14] Vampa, G., McDonald, C. R., Orlando, G., Corkum, P. B., and Brabec, T., "Semiclassical analysis of high harmonic generation in bulk crystals," *Phys. Rev. B* **91**, 064302 (Feb 2015).

[15] Schubert, O., Hohenleutner, M., Langer, F., Urbanek, B., Lange, C., Huttner, U., Golde, D., Meier, T., Kira, M., Koch, S. W., and Huber, R., "Sub-cycle control of terahertz high-harmonic generation by dynamical bloch oscillations," *Nat. Photon.* **8**, 119–123 (02 2014).

[16] Golde, D., Meier, T., and Koch, S. W., "High harmonics generated in semiconductor nanostructures by the coupled dynamics of optical inter- and intraband excitations," *Phys. Rev. B* **77**, 075330 (Feb 2008).

[17] Sudrie, L., Couairon, A., Franco, M., Lamouroux, B., Prade, B., Tzortzakis, S., and Mysyrowicz, A., "Femtosecond laser-induced damage and filamentary propagation in fused silica," *Phys. Rev. Lett.* **89**, 186601 (Oct 2002).

[18] Bergé, L., Skupin, S., Nuter, R., Kasparian, J., and Wolf, J.-P., "Ultrashort filaments of light in weakly ionized, optically transparent media," *Rep. on Prog. in Phys.* **70**(10), 1633 (2007).

[19] Vampa, G., McDonald, C. R., Orlando, G., Klug, D. D., Corkum, P. B., and Brabec, T., "Theoretical analysis of high-harmonic generation in solids," *Phys. Rev. Lett.* **113**, 073901 (Aug 2014).

[20] Zhokhov, P. A. and Zheltikov, A. M., "Field-cycle-resolved photoionization in solids," *Phys. Rev. Lett.* **113**, 133903 (Sep 2014).

[21] Földi, P., Benedict, M. G., and Yakovlev, V. S., "The effect of dynamical bloch oscillations on optical-field-induced current in a wide-gap dielectric," *New J. of Phys.* **15**(6), 063019 (2013).

[22] Keldysh, L. V., "Ionization in the field of a strong electromagnetic wave," *Sov. Phys. JETP* **20**(5), 1307 (1965).